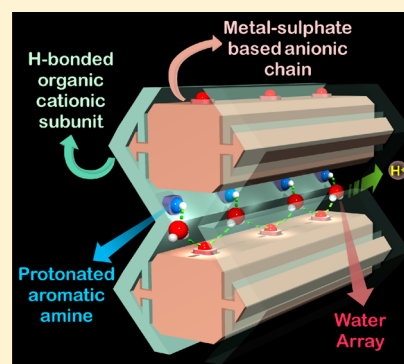


Coherent Fusion of Water Array and Protonated Amine in a Metal–Sulfate-Based Coordination Polymer for Proton Conduction

Biplab Manna,[†] Bihag Anothumakkool,^{‡,§} Aamod V. Desai,[†] Partha Samanta,[†] Sreekumar Kurungot,^{‡,§} and Sujit K. Ghosh^{*,†}[†]Department of Chemistry, Indian Institute of Science Education and Research, Dr. Homi Bhabha Road, Pashan, Pune 411 008, India[‡]Physical and Materials Chemistry Division, CSIR-National Chemical Laboratory (NCL), Pune 411 008, India[§]Academy of Scientific and Innovative Research (AcSIR), Anusandhan Bhawan, 2 Rafi Marg, New Delhi 110 001, India

S Supporting Information

ABSTRACT: A new function of metal–sulfate-based coordination polymer (CP) for proton conduction was investigated through rational integration of a continuous water array and protonated amine in the coordination space of the CP. The H-bonded arrays of water molecules along with nitrogen-rich aromatic cation (protonated melamine) facilitate proton conduction in the compound under humid conditions. Although several reports of metal–oxalate/phosphate-based CPs showing proton conduction are known, this is the first designed synthesis of a metal–sulfate-based CP bearing water arrays functioning as a solid-state proton conductor.



■ INTRODUCTION

Coordination polymers (CPs)/metal–organic frameworks (MOFs) are highly crystalline materials that manifest tailorable functions owing to facile customization of their framework structures.¹ Among various facets, proton conduction in CPs is seeking much attention in recent years on account of its potential application as solid-state electrolyte in fuel cell.² Generally proton conductivity in CPs can be obtained in two ways. In the first instance, acidic/hydrophilic functionalities are introduced into the framework externally, while by the second route the proton source and ordered carrier molecules are simultaneously present in the framework structure.^{2a} The information concerning molecular-level ion-conduction pathway can be communicated due to the complementary presence of a well-ordered network in such materials. Recently, various functional CPs have been reported as proton-conducting materials.³ Among them metal–oxalate/phosphate-based coordination polymers have been commonly studied for anhydrous and water-mediated proton conduction.⁴ Hence, for further development and comprehensive understanding of solid-state proton-conducting materials, investigation of other metal–anion-based CPs is pertinently important. Intriguingly metal–sulfate-based CPs have not been explored as solid-state proton conductors, although it is well-known about the facile formation of anionic frameworks by combining metal ions and sulfate anions.⁵ Extra framework cations are required for balancing the charge of such anionic chain.

Use of organic amine in such reaction medium can provide the extra framework cation in the form of protonated organic

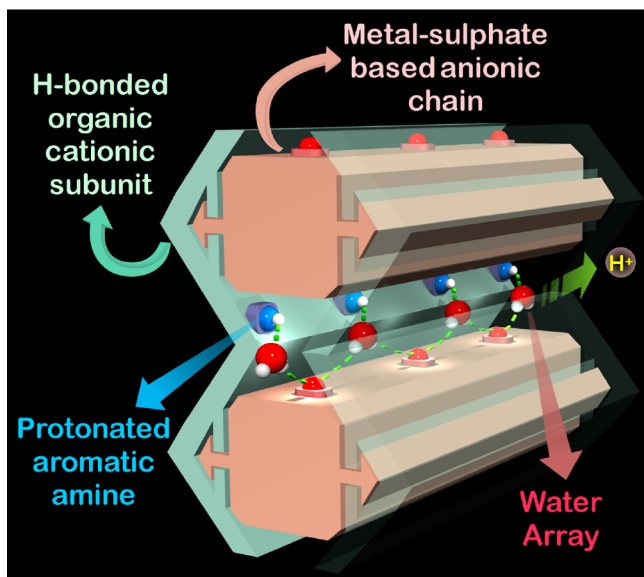
amine.⁶ In case of participation by nitrogen-rich aromatic amine, efficient movement of proton in its cationic form might be facilitated. Employment of water medium in such reactions often can lead to the entrapment of water molecules in the crystal lattice owing to hydrophilic nature of such host framework.⁷ The complementary presence of such free lattice water molecules along with nitrogen-rich aromatic protonated amine can help in formation of extensive H-bonding array of lattice water molecules along the metal–sulfate chain. This H-bonding array of water molecules in colligation with protonated aromatic amine may render an effective proton hopping pathway, which eventually can lead to fabrication of an effective solid-state proton-conducting material. Thus, such H-bonded sulfate-based CPs may find an avenue in the further development of solid-state proton conductors. Here, we chose $\text{In}_2(\text{SO}_4)_3$ –melamine and water system to develop a sulfate-based coordination polymer forming H-bonded three-dimensional (3D) network for proton conduction. Simultaneous presence of nitrogen-rich aromatic cation (protonated melamine) and continuous array of water molecules in the CP described a H-bonding pathway and thereby favors the water-assisted proton conduction in the polymer (Scheme 1). To the best of our knowledge, this is the first report of metal–sulfate-based CP carrying a continuous water array functioning as a solid-state proton conductor.

Received: February 20, 2015

Published: May 18, 2015



Scheme 1. Schematic Overview of H-Bonded Metal–Sulfate-Based Coordination Polymer for Water-Mediated Proton Conduction



EXPERIMENTAL SECTION

Materials and Measurements. All the reagents and solvents were commercially available and used without further purification. Powder X-ray diffraction (PXRD) patterns were measured on Bruker D8 Advanced X-ray diffractometer at room temperature using Cu $K\alpha$ radiation ($\lambda = 1.5406 \text{ \AA}$) with a scan speed of $0.5^\circ \text{ min}^{-1}$ and a step size of 0.01° in 2θ . Thermogravimetric analysis (TGA) was recorded on PerkinElmer STA 6000 TGA analyzer under N_2 atmosphere with heating rate of 10° C/min . The IR spectra were recorded on a ThermoScientific–Nicolet-6700 FT-IR spectrometer. FT-IR spectra were recorded on NICOLET 6700 FT-IR Spectrophotometer using KBr Pellets.

Synthesis of Compound 1. Single crystals of compound **1** were synthesized by reacting $\text{In}_2(\text{SO}_4)_3$ (0.0427 g, 0.0825 mmol), melamine (0.0315 g, 0.25 mmol) in H_2O (2 mL), and 1-butanol (1 mL) in a 5 mL screw-capped vial. The vial was heated to 110° C for 26 h under autogenous pressure and then cooled to room temperature over 14 h. The colorless rod-shaped single crystals of compound **1** were obtained with ~70% yield.

X-ray Structural Studies. Single-crystal X-ray data of compound **1** were collected at 100 K on a Bruker KAPPA APEX II CCD Duo diffractometer (operated at 1500 W power: 50 kV, 30 mA) using graphite-monochromated Mo $K\alpha$ radiation ($\lambda = 0.71073 \text{ \AA}$). Crystal was on nylon CryoLoops (Hampton Research) with Paratone-N (Hampton Research). The data integration and reduction were processed with SAINT¹⁰ software. A multiscan absorption correction was applied to the collected reflections. The structure was solved by the direct method using SHELXTL¹¹ and was refined on F^2 by full-matrix least-squares technique using the SHELXL-97¹² program package within the WINGX¹³ program. All non-hydrogen atoms were refined anisotropically. All hydrogen atoms were located in successive difference Fourier maps, and they were treated as riding atoms using SHELXL default parameters. The structures were examined using the Adsym subroutine of PLATON¹⁴ to ensure that no additional symmetry could be applied to the models.

Impedance Analysis. Impedance analysis of the samples was performed in Bio-Logic VMP-3. Measurements were done in a two-electrode assembly with stainless steel discs as electrode, and samples were kept in between them in the form of solid pellets by applying a spring load of 0.5 N/m^2 . The whole cell assembly was kept in Espec environmental test chamber to control the temperature and humidity. Applied frequency range for the measurement was from 1×10^6 to

0.01 Hz against the open-circuit potential with sinus amplitude of 10 mV . All the electrochemical impedance spectroscopy (EIS) data were fitted using an EC-Lab Software V10.19.

RESULTS AND DISCUSSION

Reaction of melamine (L) with $\text{In}_2(\text{SO}_4)_3$ in water medium under solvothermal condition gave rod-shaped colorless single crystals of compound **1** $[\{\text{In}_2(\mu\text{-OH})_2(\text{SO}_4)_4\} \cdot \{(\text{LH})_4\} \cdot n\text{H}_2\text{O}]_n$. LH represents protonated melamine (Figure 1).

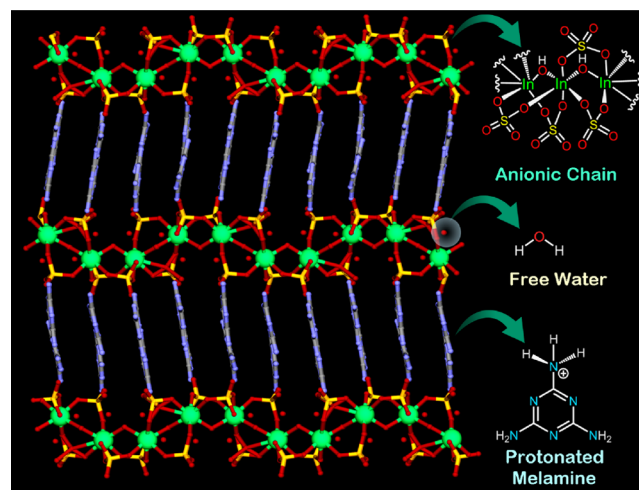


Figure 1. Overall packing of compound **1** along a axis showing anionic chain, protonated melamine, and free water molecules.

Single-crystal analysis of the compound revealed the generation of one-dimensional (1D) anionic coordination polymer chain, which are further hydrogen-bonded with protonated aromatic amine and lattice water molecules to render H-bonded 3D network with 1D pore channel along b axis (Figure 2A).

A single-crystal X-ray diffraction (SC-XRD) study of the compound showed crystallization in monoclinic crystal system with space group $P2_1/n$. An asymmetric unit of the compound **1** is made of anionic chain $[\{\text{In}_2(\mu\text{-OH})_2(\text{SO}_4)_4\}]^{4-}$, organic cationic amine $[(\text{LH})_4]^{4+}$, and free lattice water molecules. Each metal center is octahedrally connected to six oxygen donor atoms. Out of six O-donor atoms, four of them come from four sulfate groups, and rest of them are bridging hydroxy groups. The anionic subunit of the asymmetric unit consists of four SO_4^{2-} , two OH^- , and two In metal centers and contains overall tetranegative charge on it (4^-). Hence each In metal center shows +3 oxidation state to make overall asymmetric unit neutral. Each In(III) exhibits distorted octahedral geometry by the coordination of four sulfate oxygen atoms (three equatorial and one axial) and two hydroxy oxygen atoms (one equatorial, one axial). Each sulfate ion connects two adjacent metal centers via two oxygens of it in a bidentate fashion. Thus, ligation of SO_4^{2-} in bidentate manner along with μ -hydroxy coordination creates 1D anionic chain of $[\{\text{In}_2(\mu\text{-OH})_2(\text{SO}_4)_4\}]_n^{4-}$.

These 1D anionic chains form extensive H-bond with organic cationic ammine and free lattice water molecules to create H-bonded CP. Free water molecules in the compound also form H-bonding 1D array in between two adjacent anionic chains (Figure 2B). PXRD patterns of ground sample matched well with its simulated patterns, indicating bulk-phase purity of compound **1** (Figure 3). TGA of powder sample of compound **1** suggested a continuous initial loss due to the presence of

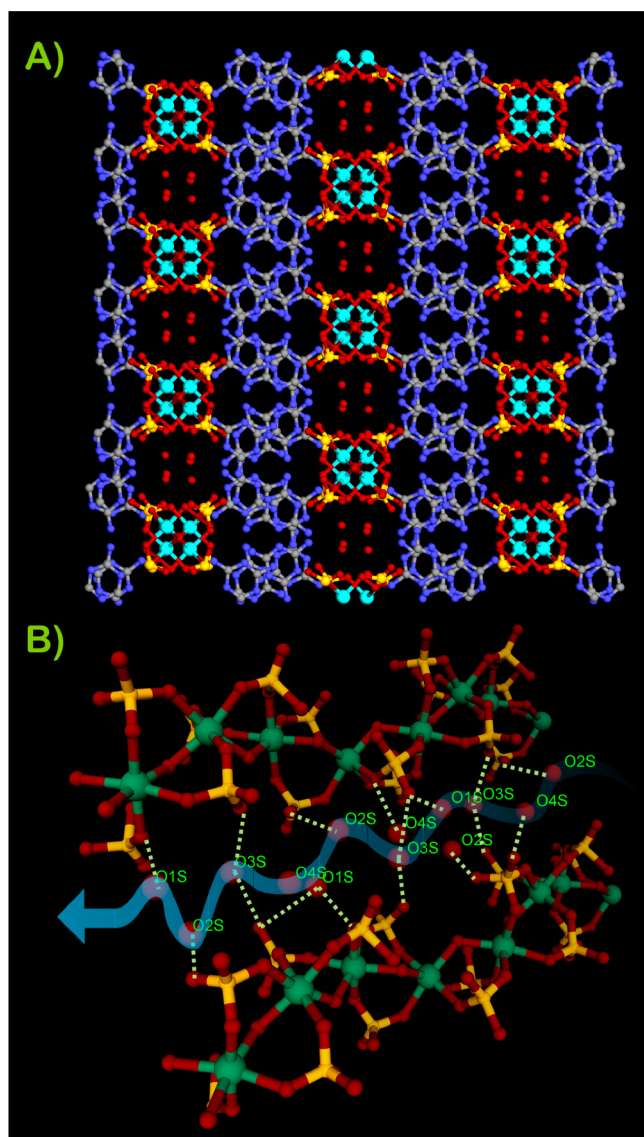


Figure 2. (A) Overall packing of compound 1. (B) Hydrogen-bonded water molecules chain in compound 1.

strongly hydrogen-bonded water molecules in the structure (Figure 4). Structural integrity of the compound 1 was maintained even at elevated temperatures as revealed by variable-temperature PXRD diffraction patterns (Figure 5). The extensive H-bonded network present in the above-mentioned coordination polymer is crucial and often required for proton conduction. Hence, the H-bonded 3D network composed of metal–sulfate-based anionic chain and protonated melamine with continuous array of water molecules may act as a potential proton conducting material.

Very recently portable fuel cells that work in low temperatures and humidified conditions are seeking much attention as clean energy sources. Proton conductivity of compound 1 was measured by using EIS technique by controlling humidity as well as temperature. Nyquist plot of the compound 1 measured at 98% relative humidity (RH) and 30 °C is shown in Figure 6. A semicircle at the high-frequency region represents the bulk electrolyte resistance in parallel with a constant phase element (CPE) as found by fitting the EIS spectra (details are given in the Supporting Information). While at the low-frequency region the tail indicates the diffusion resistance of the mobile

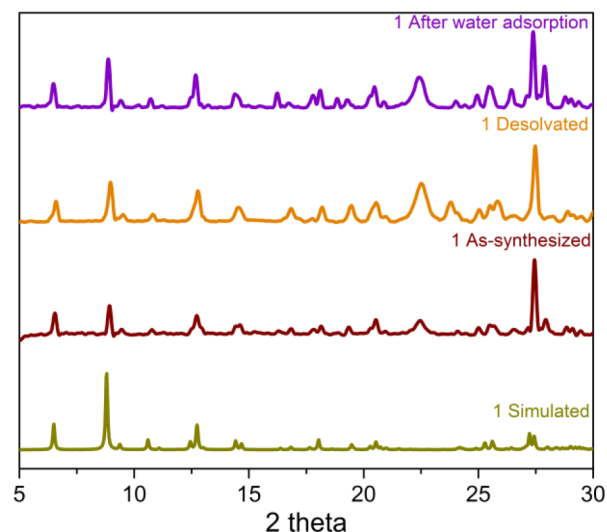


Figure 3. PXRD patterns of simulated, as-synthesized, desolvated, and post-water adsorption phases of compound 1.

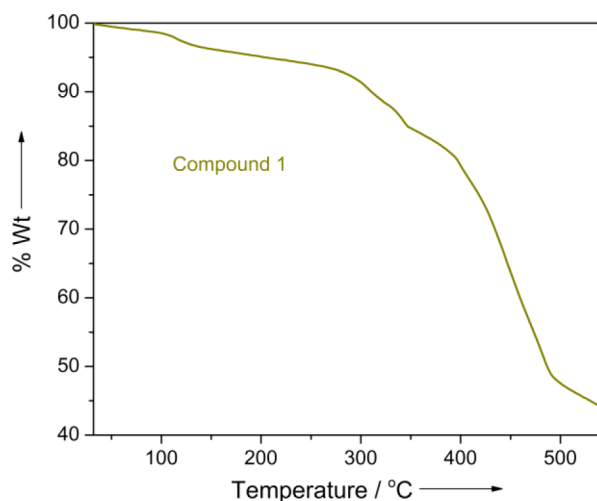


Figure 4. TGA plot of compound 1.

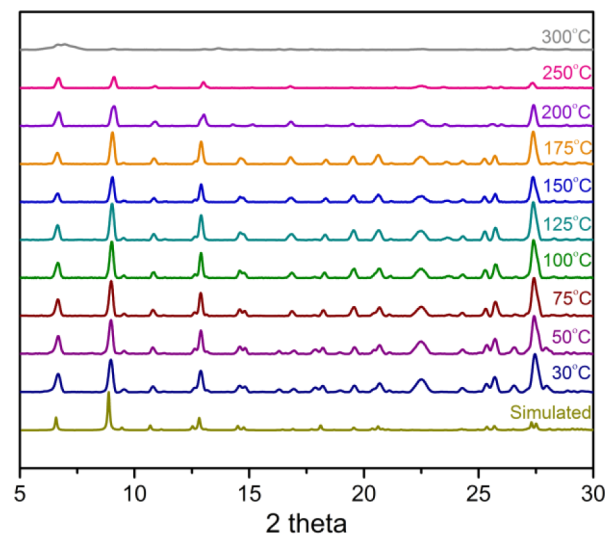


Figure 5. Variable-temperature PXRD patterns of compound 1.

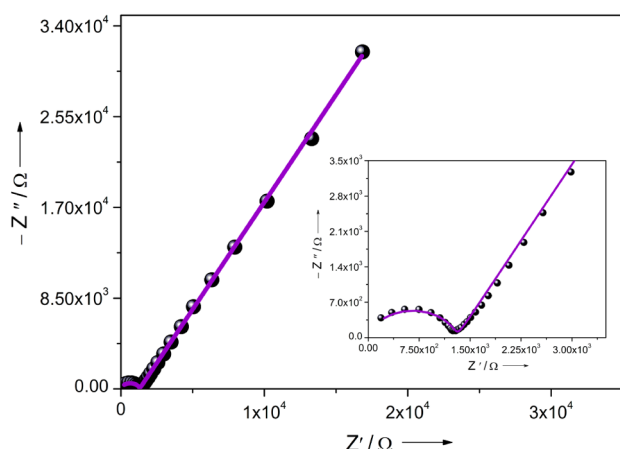


Figure 6. Nyquist plot of compound **1** at 98% RH and 30°C. (inset) Narrowed high-frequency region.

ions at the electrode–electrolyte interface. From the varied humidity-dependent EIS measurements it is found that compound **1** shows humidity-dependent conductivity, where at 50%RH, conductivity was on the order of $1 \times 10^{-7} \text{ S cm}^{-1}$ (Supporting Information, Figure S9). Conductivity is found to be increasing as expected with increasing humidity and reached 1.0×10^{-5} at 95% RH (Figure S9). The conductivity became maximum at 98% RH with the value of $4.4 \times 10^{-5} \text{ S cm}^{-1}$ (Figure 6). It is worth noting that conductivity of compound **1** increases gradually with increase in humidity to 95% RH, but a sudden jump in conductivity at 98% RH is observed (Figure 7).

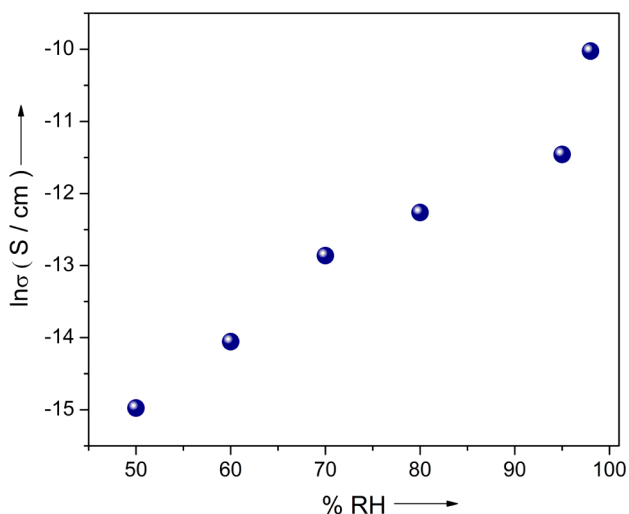


Figure 7. Conductivity vs %RH of compound **1** at 30°C.

Such increase in conductivity beyond 95% RH may be attributed to the presence of large number of water molecules for extensive H-bonding array in the framework at saturated humidification. The trend in conductivity as observed in impedance analysis of compound **1** was also supported from the water-adsorption profile of compound **1** at 298 K (Supporting Information, Figure S11). Water-adsorption profile of compound **1** indicates stepwise water uptake, which is in good agreement with sudden increase in conductivity beyond 95% RH (Figure S11). The conductivity of this compound under humid condition is comparatively better than the similarly hydrogen-bonded compound $[(\text{C}_6\text{H}_{10}\text{N}_2)_2(\text{SO}_4)_2 \cdot$

$3\text{H}_2\text{O}]_n$ consisting of phenylene diamine dication, sulfate anion, and water.⁸ To get the activation energy (E_a) for the proton conduction, temperature dependence conductivity was measured at 95% RH (Supporting Information, Figure S8). The E_a was measured to be 0.316 eV from the Arrhenius plot (Figure 8), which is quite low value suggesting that probably

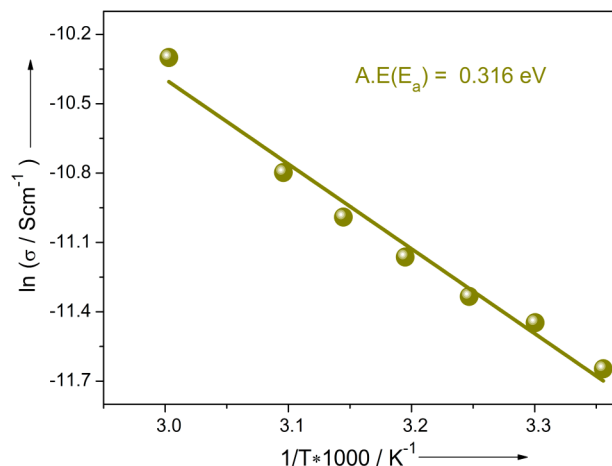


Figure 8. Arrhenius plot for temperature dependence of conductivity at 95% RH of compound **1**.

Grotthuss mechanism is operating for proton hopping.^{2a,9} We also performed impedance analysis of the compound under D_2O atmosphere. At 98% RH the conductivity in the presence of D_2O became $1.01 \times 10^{-5} \text{ S cm}^{-1}$, which is quite low as compared to H_2O condition (Supporting Information, Figure S10). This measurement under D_2O atmosphere further confirmed the water-assisted proton conduction in the compound. The protonated melamine behaves as a feasible proton source, which is further hydrogen-bonded with the ordered extended H-bonded water molecules chain that favors the proton-transport phenomena in this compound. With increase in humidity, concentration of carrier molecules increases, which results in elevation in conductivity. At saturated humidification, high carrier concentration in the compound may be effective for efficient proton conduction.

CONCLUSION

To conclude, we have successfully synthesized a novel metal–sulfate-based coordination polymer forming H-bonded 3D network by rational confinement of nitrogen-rich protonated aromatic cations (protonated melamine) and array of water molecules for solid-state proton conduction. The compound shows water-mediated proton conduction owing to such extensive H-bonded network of free water molecules along with aromatic protonated amine present in the compound. Such metal–sulfate-based coordination polymers may seek greater attention in the near future toward the further development of solid-state electrolytes.

ASSOCIATED CONTENT

Supporting Information

Synthesis of compound **1**, methods of PXRD and TGA measurements, impedance analysis, crystal structures, PXRD and TGA data, IR and impedance spectra, water adsorption profile, bond lengths and angles of compound **1**, tabulated crystallographic data, and crystal structure data in CIF format.

The Supporting Information is available free of charge on the ACS Publications website at DOI: 10.1021/acs.inorgchem.5b00416.

AUTHOR INFORMATION

Corresponding Author

*Fax: +91 20 2590 8186. E-mail: sghosh@iiserpune.ac.in.

Notes

The authors declare no competing financial interest.

ACKNOWLEDGMENTS

B.M. and B.A. are thankful to CSIR for research fellowship. P.S. is thankful to UGC for research fellowship. We are thankful to IISER Pune, DST (Project No. GAP/DST/CHE-12-0083) for the financial support. We are also thankful to DST-FIST (SR/FST/CSII-023/2012) for microfocus SC-XRD facility.

REFERENCES

- (1) (a) Zhou, H.-C.; Long, J. R.; Yaghi, O. M. *Chem. Rev.* **2012**, *112*, 673–674. (b) Horcajada, P.; Gref, R.; Baati, T.; Allan, P. K.; Maurin, G.; Couvreur, P.; Ferey, G.; Morris, R. E.; Serre, C. *Chem. Rev.* **2012**, *112*, 1232–1268. (c) Stock, N.; Biswas, S. *Chem. Rev.* **2012**, *112*, 933–969. (d) Ahnfeldt, T.; Guillou, N.; Gunzelmann, D.; Margiolaki, I.; Loiseau, T.; Ferey, G.; Senker, J.; Stock, N. *Angew. Chem., Int. Ed.* **2009**, *48*, 5163–5166. (e) Devic, T.; Serre, C. *Chem. Soc. Rev.* **2014**, *43*, 6097–6115. (f) Manna, B.; Chaudhari, A. K.; Joarder, B.; Karmakar, A.; Ghosh, S. K. *Angew. Chem., Int. Ed.* **2013**, *52*, 998–1002. (g) Manna, B.; Joarder, B.; Desai, A. V.; Karmakar, A.; Ghosh, S. K. *Chem.—Eur. J.* **2014**, *20*, 12399–12404. (h) Henke, S.; Schneemann, A.; Wütscher, A.; Fischer, R. A. *J. Am. Chem. Soc.* **2012**, *134*, 9464–9474. (i) Bétard, A.; Fischer, R. A. *Chem. Rev.* **2012**, *112*, 1055–1083. (j) Zhang, J.-W.; Zhang, H.-T.; Du, Z.-Y.; Wang, X.; Yu, S.-H.; Jiang, H.-L. *Chem. Commun.* **2014**, *50*, 1092–1094. (k) Zhang, W.; Hu, Y.; Ge, J.; Jiang, H.-L.; Yu, S.-H. *J. Am. Chem. Soc.* **2014**, *136*, 16978–16981. (l) Bloch, W. M.; Burgun, A.; Coghlan, C. J.; Lee, R.; Coote, M. L.; Doonan, C. J.; Sumby, C. J. *Nat. Chem.* **2014**, *6*, 906–912. (m) Bloch, W. M.; Sumby, C. J. *Chem. Commun.* **2012**, *48*, 2534–2536. (n) Konidaris, K. F.; Morrison, C. N.; Servetas, J. G.; Haukka, M.; Lan, Y.; Powell, A. K.; Plakatouras, J. C.; Kostakis, G. E. *CrystEngComm* **2012**, *14*, 1842–1849. (o) Gao, W.-Y.; Chen, Y.; Niu, Y.; Williams, K.; Cash, L.; Perez, P. J.; Wojtas, L.; Cai, J.; Chen, Y.-S.; Ma, S. *Angew. Chem., Int. Ed.* **2014**, *53*, 2615–2619. (p) Wang, X.-S.; Chrzanowski, M.; Gao, W.-Y.; Wojtas, L.; Chen, Y.-S.; Zaworotko, M. J.; Ma, S. *Chem. Sci.* **2012**, *3*, 2823–2827.
- (2) (a) Ramaswamy, P.; Wong, N. E.; Shimizu, G. K. H. *Chem. Soc. Rev.* **2014**, *43*, 5913–5932. (b) Yamada, T.; Otsubo, K.; Makiura, R.; Kitagawa, H. *Chem. Soc. Rev.* **2013**, *42*, 6655–6669. (c) Horike, S.; Umeyama, D.; Kitagawa, S. *Acc. Chem. Res.* **2013**, *46*, 2376–2384.
- (3) (a) Yoon, M.; Suh, K.; Natarajan, S.; Kim, K. *Angew. Chem., Int. Ed.* **2013**, *52*, 2–15. (b) Shimizu, G. K. H.; Taylor, J. M.; Kim, S. *Science* **2013**, *41*, 354–355. (c) Hurd, J. A.; Vaidhyanathan, R.; Thangadurai, V.; Ratcliffe, C. I.; Moudrakovski, I. L.; Shimizu, G. K. H. *Nat. Chem.* **2009**, *1*, 705–710. (d) Sen, S.; Nair, N. N.; Yamada, T.; Kitagawa, H.; Bharadwaj, P. K. *J. Am. Chem. Soc.* **2012**, *134*, 19432–19437. (e) Yamada, T.; Otsubo, K.; Makiura, R.; Kitagawa, H. *Chem. Soc. Rev.* **2013**, *42*, 6655–6669. (f) Shigematsu, A.; Yamada, T.; Kitagawa, H. *J. Am. Chem. Soc.* **2011**, *133*, 2034–2036. (g) Bureekaew, S.; Horike, S.; Higuchi, M.; Mizuno, M.; Kawamura, T.; Tanaka, D.; Yanai, N.; Kitagawa, S. *Nat. Mater.* **2009**, *8*, 831–836. (h) Umeyama, D.; Horike, S.; Inukai, M.; Hijikata, Y.; Kitagawa, S. *Angew. Chem., Int. Ed.* **2011**, *50*, 11706–11709. (i) Ponomareva, V. G.; Kovalenko, K. A.; Chupakhin, A. P.; Dybtsev, D. N.; Shutova, E. S.; Fedin, V. P. *J. Am. Chem. Soc.* **2012**, *134*, 15640–15643. (j) Horike, S.; Umeyama, D.; Kitagawa, S. *Acc. Chem. Res.* **2013**, *46*, 2376–2384. (k) Horike, S.; Kamitsubo, Y.; Inukai, M.; Fukushima, T.; Umeyama, D.; Itakura, T.; Kitagawa, S. *J. Am. Chem. Soc.* **2013**, *135*, 4612–4615. (l) García, M. B.; Colodrero, R. M. P.; Papadaki, M.; Garczarek, P.; Zoń, J.; Pastor, P. O.; Losilla, E. R.; Reina, L. L.; Aranda, M. A. G.; Lazarte, D. C.; Demadis, K. D.; Cabeza, A. *J. Am. Chem. Soc.* **2014**, *136*, 5731–5739. (m) Li, S.-L.; Xu, Q. *Energy Environ. Sci.* **2013**, *6*, 1656–1683. (n) Phang, W. J.; Lee, W. R.; Yoo, K.; Ryu, D. W.; Kim, B.; Hong, C. S. *Angew. Chem., Int. Ed.* **2014**, *53*, 8383–8387. (o) Colodrero, R. M. P.; Papathanasiou, K. E.; Stavgiannoudaki, N.; Olivera-Pastor, P.; Losilla, E. R.; Aranda, M. A. G.; Leon-Reina, L.; Sanz, J.; Sobrados, I.; Choquesillo-Lazarte, D.; García-Ruiz, J. M.; Atienzar, P.; Rey, F.; Demadis, K. D.; Cabeza, A. *Chem. Mater.* **2012**, *24*, 3780–3792. (p) Colodrero, R. M. P.; Olivera-Pastor, P.; Losilla, E. R.; Aranda, M. A. G.; Leon-Reina, L.; Papadaki, M.; McKinlay, A. C.; Morris, R. E.; Demadis, K. D.; Cabeza, A. *Dalton Trans.* **2012**, *41*, 4045–4051. (q) Kim, S. R.; Dawson, K. W.; Gelfand, B. S.; Taylor, J. M.; Shimizu, G. K. H. *J. Am. Chem. Soc.* **2013**, *135*, 963–966. (r) Taylor, J. M.; Mah, R. K.; Moudrakovski, I. L.; Ratcliffe, C. I.; Vaidhyanathan, R.; Shimizu, G. K. H. *J. Am. Chem. Soc.* **2010**, *132*, 14055–14057. (s) Taylor, J. M.; Dawson, K. W.; Shimizu, G. K. H. *J. Am. Chem. Soc.* **2013**, *135*, 1193–1196. (t) Parshamoni, S.; Jena, H. S.; Sanda, S.; Konar, S. *Inorg. Chem. Front.* **2014**, *1*, 611–620. (u) Sen, S.; Yamada, T.; Kitagawa, H.; Bharadwaj, P. K. *Cryst. Growth Des.* **2014**, *14*, 1240–1244. (v) Dybtsev, D. N.; Ponomareva, V. G.; Aliev, S. B.; Chupakhin, A. P.; Gallyamov, M. R.; Moroz, N. K.; Kolesov, B. A.; Kovalenko, K. A.; Shutova, E. S.; Fedin, V. P. *ACS Appl. Mater. Interfaces* **2014**, *6*, 5161–5167.
- (4) (a) Nagarkar, S. S.; Unni, S. M.; Sharma, A.; Kurungot, S.; Ghosh, S. K. *Angew. Chem., Int. Ed.* **2014**, *53*, 2638–2642. (b) Yamada, T.; Sadakiyo, M.; Kitagawa, H. *J. Am. Chem. Soc.* **2009**, *131*, 3144–3145. (c) Horike, S.; Chen, W.; Itakura, T.; Inukai, M.; Umeyama, D.; Asakura, H.; Kitagawa, S. *Chem. Commun.* **2014**, *50*, 10241–10243. (d) Inukai, M.; Horike, S.; Chen, W.; Umeyama, D.; Itakura, T.; Kitagawa, S. *J. Mater. Chem. A* **2014**, *2*, 10404–10409. (e) Sadakiyo, M.; Yamada, T.; Kitagawa, H. *J. Am. Chem. Soc.* **2009**, *131*, 9906–9907. (f) Sadakiyo, M.; Okawa, H.; Shigematsu, A.; Ohba, M.; Yamada, T.; Kitagawa, H. *J. Am. Chem. Soc.* **2012**, *134*, 5472–5475. (g) Okawa, H.; Shigematsu, A.; Sadakiyo, M.; Miyagawa, T.; Yoneda, K.; Ohba, M.; Kitagawa, H. *J. Am. Chem. Soc.* **2009**, *131*, 13516–13522. (h) Horike, S.; Umeyama, D.; Inukai, M.; Itakura, T.; Kitagawa, S. *J. Am. Chem. Soc.* **2012**, *134*, 7612–7615. (i) Umeyama, D.; Horike, S.; Inukai, M.; Kitagawa, S. *J. Am. Chem. Soc.* **2013**, *135*, 11345–11350. (j) Umeyama, D.; Horike, S.; Inukai, M.; Itakura, T.; Kitagawa, S. *J. Am. Chem. Soc.* **2012**, *134*, 12780–12785.
- (5) (a) Choudhury, A.; Krishnamoorthy, J.; Rao, C. N. R. *Chem. Commun.* **2001**, 2610–2611. (b) Paul, G.; Choudhury, A.; Rao, C. N. R. *J. Chem. Soc., Dalton Trans.* **2002**, 3859–3867. (c) Doran, M.; Norquist, A. J.; O'Hare, D. *Chem. Commun.* **2002**, 2946–2947. (d) Bharara, M. S.; Gorden, A. E. V. *Dalton Trans.* **2010**, *39*, 3557–3559. (e) Zheng, L.; Qiu, X.; Xu, Y.; Fu, J.; Yuan, Y.; Zhu, D.; Chen, Su. *CrystEngComm* **2011**, *13*, 2714–2720. (f) Paul, A. K.; Sanyal, U.; Natarajan, S. *Cryst. Growth Des.* **2010**, *10*, 4161–4175. (g) Norquist, A. J.; Thomas, P. M.; Doran, M. B.; O'Hare, D. *Chem. Mater.* **2002**, *14*, 5179–5184.
- (6) (a) Yotnoi, B.; Rujiwattra, A.; Reddy, M. L. P.; Sarma, D.; Natarajan, S. *Cryst. Growth Des.* **2011**, *11*, 1347–1356. (b) Doran, M. B.; Norquist, A. J.; O'Hare, D. *Inorg. Chem.* **2003**, *42*, 6989–6995.
- (7) (a) Fu, Y.; Xu, Z.; Ren, J.; Wu, H.; Yuan, R. *Inorg. Chem.* **2006**, *45*, 8452–8458. (b) Ramaswamy, P.; Hegde, N. N.; Prabhu, R.; Vidya, V.; Datta, M. A.; Natarajan, S. *Inorg. Chem.* **2009**, *48*, 11697–11711.
- (8) Xu, H.-R.; Zhang, Q.-C.; Zhao, H.-X.; Long, L.-S.; Huang, R.-B.; Zheng, L.-S. *Chem. Commun.* **2012**, *48*, 4875–4877.
- (9) (a) Marx, D.; Tuckerman, M. E.; Hutter, J.; Parrinello, M. *Nature* **1999**, *397*, 601–604. (b) van Grothuss, C. J. T. *Ann. Chim.* **1806**, *58*, 54–73. (c) Atkins, P.; de Paula, J. *Physical Chemistry*, 8th ed.; Oxford University Press: Oxford, U.K., 2006; Ch. 21.7, p 766.
- (10) SAINT Plus, Version 7.03; Bruker AXS Inc.: Madison, WI, 2004.
- (11) Sheldrick, G. M. *SHELXTL Reference Manual*, Version 5.1; Bruker AXS: Madison, WI, 1997.
- (12) Sheldrick, G. M. *Acta Crystallogr., Sect. A* **2008**, *112*.
- (13) Farrugia, L. *WINGX*, Version 1.80.05; University of Glasgow: Glasgow, Scotland, 2013.

(14) Spek, A. L. *PLATON*, A Multipurpose Crystallographic Tool; Utrecht University: Utrecht, The Netherlands, 2005.